

SPATIAL GRAPH SIGNAL INTERPOLATION WITH AN APPLICATION FOR MERGING BCI DATASETS WITH VARIOUS DIMENSIONALITIES

Yassine El Ouahidi, Lucas Drumetz, Giulia Lioi, Nicolas Farrugia, Bastien Pasdeloup and Vincent Gripon

IMT Atlantique, Lab-STICC, UMR CNRS 6285, F-29238 Brest, France, name.surname@imt-atlantique.fr

ABSTRACT

BCI Motor Imagery datasets usually are small and have different electrodes setups. When training a Deep Neural Network, one may want to capitalize on all these datasets to increase the amount of data available and hence obtain good generalization results. To this end, we introduce a spatial graph signal interpolation technique, that allows to interpolate efficiently multiple electrodes. We conduct a set of experiments with five BCI Motor Imagery datasets comparing the proposed interpolation with spherical splines interpolation. We believe that this work provides novel ideas on how to leverage graphs to interpolate electrodes and on how to homogenize multiple datasets.

Index Terms— graph signal processing, BCI, EEG, motor imagery, signal interpolation, DNN

1. INTRODUCTION

One important challenge in brain signals classification is the lack of large, homogeneous datasets, such as those available in computer vision. This is also true for Brain Computer Interfaces (BCI) where usually the electroencephalographic (EEG) signal is collected from a few subjects with specific recording setups (electrodes layout, sampling frequency, stimulation paradigm). The lack of training data also explain why only recently methods based on deep learning and transfer learning have been applied to BCI signal decoding, with contrasting results [1]. One way to tackle this limitation is to setup a joint analysis on datasets. Such solutions usually rely on hand-crafted features based on physiological priors or hardly interpretable deep learning models. In this paper, we propose a new method for merging EEG datasets based on graph signal interpolation and show an application to BCI Motor Imagery (MI) classification. A graph is learned from EEG data and a graph signal interpolation technique is implemented to obtain a unified, virtual, electrodes setup. This method does not require any prior and provides interpretable results in terms of EEG spatial patterns.

2. RELATED WORK

2.1. BCI MI classification

BCI systems are based on the real-time measure of brain signals (typically EEG) and usually need an offline training phase during which the system is calibrated; then during the operational phase the system classifies brain activity patterns and translates them into commands for a device in real-time. In current applications, a training dataset needs to be pre-recorded from the user to have reliable systems, due to the lack of classifiers able to generalise across subjects and EEG setups [1]. To go towards calibration-free, high accuracy BCI systems, a key feature is the ability to efficiently extract knowledge from the variety of datasets available in literature and transfer it to new subjects. However, the great majority of the works in literature consider separate BCI datasets [2, 3].

Recently, an attempt to exploit information jointly from different EEG datasets has been made with the NeurIPS EEG Transfer learning challenge BEETL [4]. This challenge aims at developing algorithms to transfer knowledge between different subjects and EEG datasets and at defining a new benchmark for EEG signals classification. In this challenge, three source MI datasets are provided, and algorithms are then tested on two unseen datasets. In order to train a unique model on the ensemble of the source MI datasets, a first step is to integrate data from different setups. In the context of the challenge, simple solutions such as considering common electrodes (intersection) were proposed, which totally disregards information of the dropped electrodes. Here we propose a methodology that exploits information from all the available electrodes based on graph signal interpolation.

2.2. Graph Signal Processing

An intuitive way to represent interactions between electrodes in BCI context is to use spatial graphs. EEG signals can then be seen as observations over this graph, with an added temporal dimension. Graph Signal Processing (GSP) then offers the tools to process such signals [5, 6]. In the context of MI decoding, the use of GSP-based methods also brings forward interpretability questions. In this setting, a weighted graph $\mathcal{G} = \langle \mathcal{V}, \mathcal{E} \rangle$ with vertices \mathcal{V} and edges $\mathcal{E} \subset \mathcal{V} \times \mathcal{V}$ is used to model electrodes and their interactions. Such a graph

Thanks to the Brittany region for its support.

can be equivalently represented by a symmetric weights matrix $\mathbf{W} \in \mathbb{R}^{|\mathcal{V}| \times |\mathcal{V}|}$ such that $W_{ij} = 0$ if $\{i, j\} \notin \mathcal{E}$. We then note $\mathbf{D} \in \mathbb{R}^{|\mathcal{V}| \times |\mathcal{V}|}$ the degrees matrix of \mathcal{G} , such that $D_{ij} = \sum_{k=1}^{|\mathcal{V}|} W_{ik}$ if $i = j$ and 0 otherwise. From these two matrices, we can compute the Laplacian $\mathbf{L} = \mathbf{D} - \mathbf{W}$ of \mathcal{G} . Since \mathbf{L} is real and symmetric, it can be diagonalized as $\mathbf{L} = \mathbf{U}\mathbf{\Lambda}\mathbf{U}^\top$, where \mathbf{U} is a matrix of orthonormal vectors associated with eigenvalues forming the diagonal matrix $\mathbf{\Lambda}$, sorted in increasing order. A signal $\mathbf{s} \in \mathbb{R}^N$ on \mathcal{G} is an observation on each of its vertices. Its Graph Fourier Transform $\hat{\mathbf{s}} = \text{GFT}(\mathbf{s}) = \mathbf{U}^\top \mathbf{s}$ can be seen as an observation for each graph frequency. Using those elements we can define the total graph signal variation $\sigma(\mathbf{s})$ of a signal \mathbf{s} as:

$$\sigma(\mathbf{s}) = \mathbf{s}^\top \mathbf{L} \mathbf{s} = \sum_{i=1}^{|\mathcal{V}|} \Lambda_{ii} \hat{s}_i^2 = \sum_{i=1}^{|\mathcal{V}|} \sum_{j=1}^{|\mathcal{V}|} W_{ij} (s_i - s_j)^2 \quad (1)$$

2.3. Interpolation of EEG Signals

Interpolating electrodes is a common step in many EEG preprocessing pipelines and is usually needed to artificially repair the signal from noisy electrodes or trials. Multiple methods allow to perform spatial interpolation without using graphs. The reference method, implemented in many pipelines, is the Spherical Spline interpolation [7] with Legendre polynomials. Other methods use signal correlation [8] or deep learning, like [9] which is using a deep learning generator, or [10] with a deep convolutional network. However, these methods suffer from either high reconstruction error or lack of interpretability. Other methods allow to perform interpolation with the help of graphs, like the work of [11], where structural and functional connectivities are used along with a deep graph convolutional network. Their method is designed to interpolate in multiple dimensions (frequency, spatial and temporal). Other works try to optimize a graph signal criterion, like sparsity [12], or a non smooth criterion [13], but the last method is designed to perform temporal interpolation.

2.4. Homogenizing BCI datasets

Few approaches have been explored to solve the problem introduced in Section 2.1 of exploiting information jointly from different EEG datasets. In general, datasets differ in several ways (e.g sampling frequency, preprocessing, recording paradigm, electrode setup). Some of these inhomogeneities can be solved by simply windowing or resampling the EEG signals, while unifying the electrode setup remains a challenge. To solve it, different methods have been proposed. The BEETL challenge [14] winners simply reduce the spatial dimension by taking the intersections of the datasets. [15] performs PCA, which also implies a loss of information. To overcome this limitation, some techniques propose to learn another representation with adversarial learning [16] while others propose to augment the spatial dimension by going into the Riemannian space [16]. We propose to increase the spatial

dimension by staying in the electrode space and interpolate the electrodes using a graph variation optimization.

3. METHODOLOGY

Our approach consists in considering each BCI dataset as a partial sampling of a virtual, larger collection of electrodes and then using a graph interpolation technique to “recover” the missing electrodes. The graph is learned from a different EEG dataset containing all electrodes. We then use this graph to homogenize the considered BCI datasets and train them altogether in a similar setup as for the BEETL challenge.

3.1. Graph Signal Interpolation

We propose a graph signal interpolation technique that consists of minimizing graph signal variation in Equation (1) while only knowing a part of the signal. We show here that this problem admits a closed form.

Consider a graph \mathcal{G} where electrodes are vertices \mathcal{V} , with Laplacian matrix $\mathbf{L} \in \mathbb{R}^{|\mathcal{V}| \times |\mathcal{V}|}$. Let $\mathbf{s} \in \mathbb{R}^{|\mathcal{V}|}$ be a signal on \mathcal{G} . In our problem, we consider that \mathbf{s} has some missing entries, due to absence of some electrodes. The set of such missing electrodes is denoted $\mathcal{M} \subset \mathcal{V}$, and its complement $\mathcal{M}^c = \mathcal{V} \setminus \mathcal{M}$. We note $\mathbf{s}_{\mathcal{M}^c} = \{s_{i \in \mathcal{M}^c}\}$ the observed part of \mathbf{s} , and $\mathbf{s}_{\mathcal{M}} = \{s_{i \in \mathcal{M}}\}$ its missing part. We note $\mathbf{L}_{\mathcal{M}} \in \mathbb{R}^{|\mathcal{M}| \times |\mathcal{M}|}$ the submatrix of \mathbf{L} where we only keep the rows and columns with indices in \mathcal{M} , and $\mathbf{L}_{\mathcal{M}\mathcal{M}^c} \in \mathbb{R}^{|\mathcal{M}| \times |\mathcal{M}^c|}$ the submatrix of \mathbf{L} where we only keep the rows with indices in \mathcal{M} , and the columns with indices in \mathcal{M}^c .

Proposition 1. *The solution $\mathbf{s}_{\mathcal{M}}$ that optimizes the variation problem Equation (1) in our setup is directly given by the following closed form:*

$$\mathbf{s}_{\mathcal{M}} = -\mathbf{L}_{\mathcal{M}}^{-1} \mathbf{L}_{\mathcal{M}\mathcal{M}^c} \mathbf{s}_{\mathcal{M}^c} \quad (2)$$

Proof. We start from:

$$\sigma(\mathbf{s}) = \mathbf{s}^\top \mathbf{L} \mathbf{s} = \sum_{i=1}^{|\mathcal{V}|} \sum_{j=1}^{|\mathcal{V}|} s_i L_{ij} s_j \quad (3)$$

We can decompose Equation (3) into 4 terms: 1. $i \in \mathcal{M}$ and $j \in \mathcal{M}$; 2. $i \in \mathcal{M}$ and $j \notin \mathcal{M}$; 3. $i \notin \mathcal{M}$ and $j \in \mathcal{M}$; 4. $i \notin \mathcal{M}$ and $j \notin \mathcal{M}$. In our setup 2. and 3. are symmetric, and 4. is a constant. So we have:

$$\sigma(\mathbf{s}) = \mathbf{s}_{\mathcal{M}}^\top \mathbf{L}_{\mathcal{M}} \mathbf{s}_{\mathcal{M}} + 2 \sum_{i \in \mathcal{M}} \sum_{j \notin \mathcal{M}} s_i L_{ij} s_j + \text{constant}, \quad (4)$$

where $\sigma_{\mathcal{M}\mathcal{M}^c}(\mathbf{s}) = 2 \sum_{i \in \mathcal{M}} \sum_{j \notin \mathcal{M}} s_i L_{ij} s_j$ corresponds to the two symmetric parts 2. and 3. in Equation (4). We have:

$$\forall i \in \mathcal{M}, \frac{\partial \sigma_{\mathcal{M}\mathcal{M}^c}}{\partial s_i} = 2 \sum_{j \notin \mathcal{M}} L_{ij} s_j = 2(\mathbf{L}_{\mathcal{M}\mathcal{M}^c} \mathbf{s}_{\mathcal{M}^c})_i, \quad (5)$$

where we denote as $(\cdot)_i$ the i^{th} entry of the vector in parentheses. We then obtain:

$$\nabla \sigma(\mathbf{s}_{\mathcal{M}}) = 2(\mathbf{L}_{\mathcal{M}}\mathbf{s}_{\mathcal{M}} + \mathbf{L}_{\mathcal{M} \setminus \mathcal{M}}\mathbf{s}_{\mathcal{M}}) = 0 \Rightarrow \mathbf{s}_{\mathcal{M}} = -\mathbf{L}_{\mathcal{M}}^{-1}\mathbf{L}_{\mathcal{M} \setminus \mathcal{M}}\mathbf{s}_{\mathcal{M}} \quad (6)$$

Reconstructing entries in \mathcal{M} therefore requires the use of a graph. To do so, we propose to learn it from EEG signals. \square

3.2. Learning the graph

In order to reconstruct the missing entries \mathcal{M} in a signal, we propose to learn a graph \mathcal{G} of \mathcal{V} electrodes. We consider here three different graphs:

1. A spatial graph, where the adjacency matrix is based on the locations of the sensors. We binarize this graph based on a radius. This graph has the same benefits as the method Spherical Spline interpolation, and does not need additional data except the location of the sensors;
2. We add information on top of the spatial graph, by weighting its edges with Weighted Phase Lag Index (WPLI) [17] scores computed from a dataset featuring all the electrodes. A similar graph was proposed in [18];
3. We learn the adjacency matrix of an optimal graph by gradient descent, in order to build a graph that optimizes our signal variation problem. We use as loss function $1 - R^2$, with R^2 the coefficient of determination. At each step of the learning process, we randomly mask half of the electrodes and try to reconstruct them.

In a first step, we propose to learn the graph using a large dataset A containing all electrodes. In a second step, we use the learned graph to reconstruct missing electrodes in another dataset B. For that we experiment two ways of doing it. 1. Directly transferring, which means using the learned graph on A to reconstruct B; 2. Fine-tuning the learned graph A towards the dataset B. For this, a second phase where we jointly train using A and B is needed to adapt the graph on B. At each step, we solve two different problems. The first one is on B where, we randomly mask half of the electrodes of the dataset B and we try to reconstruct them. The second problem is on A where we mask all the electrodes which are A but not in B, and we try to reconstruct them. The loss is therefore a weighted average of the losses of the two problems (each loss is still $1 - R^2$). Doing that helps prevent overfitting on dataset B while fine tuning. It also helps to align dataset B to dataset A which will help to homogenize multiple datasets in the second set of experiments.

Usefulness of the graphs for reconstructing missing entries is evaluated on controlled problems, where we artificially mask electrodes, and evaluate the reconstruction capabilities of a given graph.

4. EXPERIMENTS

4.1. Interpolation of electrodes

We used multiple open access EEG MI datasets. Which are all available on MOABB [19]¹. The code of our experiments is also available at our Github².

MI dataset	Subjects	Electrodes	Samples	Sampling frequency	Dur.	Tasks
Schrimister [20]	14	76	13484	500 Hz	4 s.	L/R/F/R
BNCI2014 [21]	9	22	5184	160 Hz	3 s.	L/R/F/T
Cho2017 [22]	52	64	9880	160 Hz	3 s.	L/R
PhysionetMI [23]	109	62	9838	160 Hz	3 s.	L/R/F/BH/R
Zhou2016 [24]	4	14	1800	160 Hz	3 s.	L/R/F
Shin2017 [25]	29	22	1740	160 Hz	3 s.	L/R

Table 1: MI datasets considered. L = Left hand, R = Right hand, F = Feet, R = Rest, BH = Both hands

We have chosen to use the Schrimister dataset to learn the union graph. This dataset has the particularity to contain almost all of the electrodes of the datasets that we consider later in our application case. This dataset is also used to learn the optimal graph, and to compute WPLI. We take all the data available and apply a band-pass filter at [2,40] Hz. All the other datasets are used for two purposes: 1. To evaluate the performance of various interpolation techniques Section 4.1; 2. To create a similar setup than in the BEETL challenge and evaluate the performance of our interpolation method to homogenize datasets Section 4.2. In order to homogenize the 5 remaining datasets, we downsample to the lowest sampling frequency (160 Hz), use the first 3 seconds starting at the cue, and apply a [2,40] Hz band-pass filter.

We notice in Fig. 1 that the WPLI weighted graph allows to slightly better reconstruct the signal than the spatial graph. On the other hand, the Spherical Spline method is more efficient than the spatial and WPLI graph. We show that learning the graph outperforms all other graphs even with up to 57 missing electrodes. In the rest of this paper, we will therefore consider the learned graph.

We then evaluate the ability of the learned graph to reconstruct signals on the other datasets of our study. In Table 2, we observe that directly using it (the Transfer line), is not very efficient. This indicates that the graph is over-adapted to the Schrimister dataset on which it is trained. To compensate for this, we fine-tune it as described in Section 2.4 to each dataset individually.

By doing so, we prove the interest of the method that consistently outperforms (the Transfer + FT line) the Spherical Spline method, on all datasets, except BNCI where the fine tuning results are similar. In Fig. 1, we display the learned graph after it is trained on the Schrimister dataset. We observe a cluster in the Centro-Fronto-Parietal area on the right side around C4, and symmetrically on the left side around C3.

¹<http://moabb.neurotechx.com>

²https://github.com/elouayas/eeg_interpolation

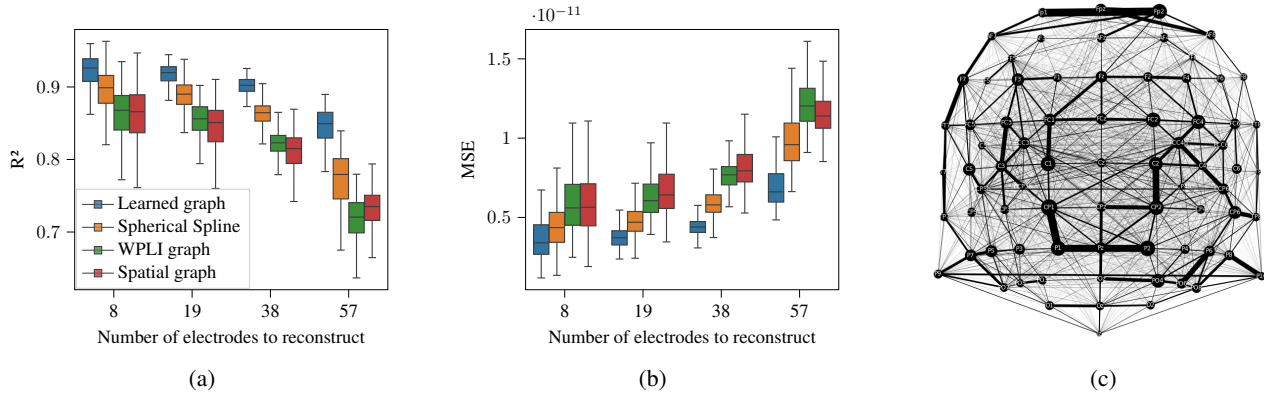


Fig. 1: (a, b) Reconstruction performances for various number of missing electrodes on Schrimister (among 76 electrodes). (c) Learned graph. The size of the nodes is weighted by their strength, and the thickness correspond to their weights. Both of them are in a square scale in order to accentuate the gaps.

Those observations make sense as those are regions and connections recruited during a motor imagery task [26].

	Physionet [23]	BNCI [21]	Cho [22]	Shin [25]	Zhou [24]
Transfer	52.5±3.6	56.3±30.4	18.8±11.8	33.8±17.3	8.3±18.1
Transfer + FT	86.1±1.2	93.2±2.8	77.1±2.3	90.4±1.7	70.0±9.2
Spatial	59.3±2.6	79.3±4.8	35.0±6.8	73.4±4.2	32.9±18.4
Spherical	80.6±4.5	94.9±1.5	75.6±4.4	85.9±4.2	54.1±21.8

Table 2: Reconstruction R^2 of half of the electrodes for various methods and various datasets

4.2. Application to multi BCI dataset training

In order to evaluate the efficiency of our interpolation method to homogenize different BCI datasets, we decided to use a setup similar to the BEETL challenge. For this, we took the same 3 source datasets (BNCI, Cho and PhysionetMI) and two new target datasets (Shin and Zhou). We use only the first 40 trials for each subjects of the two target datasets, and try to generalize to the rest of the dataset. We propose to use a deep learning model to classify our data. For this we train a 1D CNN jointly on the 4 datasets. The input of the model has for dimension the number of electrodes, so the signals of each electrode enter individually in a 1D convolution channel. The network is composed of two parts: 1. A backbone common to all datasets (with a unique entry, and multiple convolutional layers); 2. Multiple classification heads unique to each dataset (3 for the source datasets and 1 for the target dataset).

We compare through this setup the classification performances of taking only the intersection of electrodes of the 4 datasets to the performances of interpolating the missing electrodes at the intersection. We compare two way of interpolating, the first one consists in interpolating all the electrodes present in the 4 datasets and the second one consists in interpolating and selecting only the electrodes of the target dataset which is evaluated. Before training our models we align our data with Euclidean alignment [27], and resample the 4 datasets by oversampling the smaller datasets.

In Table 3, we notice that interpolating only the electrodes of the target dataset is more efficient than interpolating all the electrodes of the 4 datasets. This could be due to the fact that the information needed to classify a target dataset is contained within its electrodes, and that it is not necessary to go and get it artificially in those of the others. On the other hand it is useful to be able to exploit at least all its electrodes by interpolating the 3 source datasets. Another conclusion is that it is not always worth interpolating using our method and this procedure. If we look at the Zhou results, we see that the intersection is the one which is performing the better. This difference in results could be explained by the fact that the difference between electrodes intersection and union is very drastic for Shin, differently from Zhou.

	Shin [25]		Zhou [24]	
	Accuracy	N	Accuracy	N
Intersection	53.2±2.8	2	61.2±2.0	9
Dataset	63.2±2.3	22	56.2±4.8	14
Union	62.3±2.1	76	46.4±2.8	76

Table 3: Generalization accuracy on the two target dataset. N stands for number of electrodes. "Intersection" stands for the electrodes common to the 4 datasets. "Dataset" corresponds to the electrodes of the dataset in the column. "Union" is the union of electrodes in all 5 datasets.

5. CONCLUSION

A new and efficient electrode interpolation technique exploiting GSP tools has been proposed. We have illustrated the interest of our method to homogenize datasets. Our method allows to interpolate electrodes efficiently, and some results open new questions, especially on how one should homogenize datasets in the case where the intersection of electrodes is not reduced to its bare minimum.

6. REFERENCES

- [1] Fabien Lotte, Laurent Bougrain, Andrzej Cichocki, Maureen Clerc, Marco Congedo, Alain Rakotomamonjy, and Florian Yger, "A review of classification algorithms for eeg-based brain-computer interfaces: a 10 year update," *Journal of neural engineering*, vol. 15, no. 3, pp. 031005, 2018.
- [2] Demetres Kostas and Frank Rudzicz, "Thinker invariance: enabling deep neural networks for bci across more people," *Journal of Neural Engineering*, vol. 17, no. 5, pp. 056008, oct 2020.
- [3] Vernon J Lawhern, Amelia J Solon, Nicholas R Waytowich, Stephen M Gordon, Chou P Hung, and Brent J Lance, "Eegnet: a compact convolutional neural network for eeg-based brain-computer interfaces," *Journal of Neural Engineering*, vol. 15, no. 5, pp. 056013, jul 2018.
- [4] Xia Wei, A. Aldo Faisal, Moritz Grosse-Wentrup, Alexandre Gramfort, Sylvain Chevallier, Vinay Jayaram, Camille Jeunet, Stylianos Bakas, Siegfried Ludwig, Konstantinos Barmpas, Mehdi Bahri, Yannis Panagakis, Nikolaos A. Laskaris, Dimitrios A. Adamos, Stefanos Zafeiriou, William Duong, Stephen M. Gordon, Vernon J. Lawhern, Maciej Śliwowski, Vincent Rouanne, and Piotr Tempczyk, "2021 beel competition: Advancing transfer learning for subject independence & heterogenous eeg data sets," *ArXiv*, vol. abs/2202.12950, 2021.
- [5] David I Shuman, Sunil K Narang, Pascal Frossard, Antonio Ortega, and Pierre Vandergheynst, "The emerging field of signal processing on graphs: Extending high-dimensional data analysis to networks and other irregular domains," *IEEE signal processing magazine*, vol. 30, no. 3, pp. 83–98, 2013.
- [6] Antonio Ortega, Pascal Frossard, Jelena Kovačević, José MF Moura, and Pierre Vandergheynst, "Graph signal processing: Overview, challenges, and applications," *Proceedings of the IEEE*, vol. 106, no. 5, pp. 808–828, 2018.
- [7] François Perrin, Jacques Pernier, O Bertrand, and Jean Francois Echallier, "Spherical splines for scalp potential and current density mapping," *Electroencephalography and clinical neurophysiology*, vol. 72, no. 2, pp. 184–187, 1989.
- [8] AG Ramakrishnan and JV Satyanarayana, "Reconstruction of eeg from limited channel acquisition using estimated signal correlation," *Biomedical Signal Processing and Control*, vol. 27, pp. 164–173, 2016.
- [9] Isaac A Corley and Yufei Huang, "Deep eeg super-resolution: Upsampling eeg spatial resolution with generative adversarial networks," in *2018 IEEE EMBS International Conference on Biomedical & Health Informatics (BHI)*. IEEE, 2018, pp. 100–103.
- [10] Moonyoung Kwon, Sangjun Han, Kiwoong Kim, and Sung Chan Jun, "Super-resolution for improving eeg spatial resolution using deep convolutional neural network—feasibility study," *Sensors*, vol. 19, no. 23, pp. 5317, 2019.
- [11] Yunbo Tang, Dan Chen, Honghai Liu, Chang Cai, and Xiaoli Li, "Deep eeg superresolution via correlating brain structural and functional connectivities," *IEEE Transactions on Cybernetics*, 2022.
- [12] Pierre Humbert, Laurent Oudre, and Nicolas Vayatis, "Subsampling of multivariate time-vertex graph signals," in *2019 27th European Signal Processing Conference (EUSIPCO)*. IEEE, 2019, pp. 1–5.
- [13] Antoine Mazarguil, Laurent Oudre, and Nicolas Vayatis, "Non-smooth interpolation of graph signals," *Signal Processing*, vol. 196, pp. 108480, 2022.
- [14] Xiaoxi Wei, A. Aldo Faisal, Moritz Grosse-Wentrup, Alexandre Gramfort, Sylvain Chevallier, Vinay Jayaram, Camille Jeunet, Stylianos Bakas, Siegfried Ludwig, Konstantinos Barmpas, et al., "2021 beel competition: Advancing transfer learning for subject independence & heterogenous eeg data sets," *arXiv preprint arXiv:2202.12950*, 2022.
- [15] Thu Nguyen, Rabindra Khadka, Nhan Phan, Anis Yazidi, Pål Halvorsen, and Michael A Riegler, "Combining datasets to increase the number of samples and improve model fitting," *arXiv preprint arXiv:2210.05165*, 2022.
- [16] David Bethge, Philipp Hallgarten, Ozan Özdenizci, Ralf Mikut, Albrecht Schmidt, and Tobias Grosse-Puppenthal, "Exploiting multiple eeg data domains with adversarial learning," *arXiv preprint arXiv:2204.07777*, 2022.
- [17] Martin Vinck, Robert Oostenveld, Marijn Van Wingerden, Francesco Battaglia, and Cyriel MA Pennartz, "An improved index of phase-synchronization for electrophysiological data in the presence of volume-conduction, noise and sample-size bias," *Neuroimage*, vol. 55, no. 4, pp. 1548–1565, 2011.
- [18] Mathilde Ménoret, Nicolas Farrugia, Bastien Pasdeloup, and Vincent Gripon, "Evaluating graph signal processing for neuroimaging through classification and dimensionality reduction," in *2017 IEEE Global Conference on Signal and Information Processing (GlobalSIP)*. IEEE, 2017, pp. 618–622.
- [19] Vinay Jayaram and Alexandre Barachant, "Moabb: trustworthy algorithm benchmarking for bcis," *Journal of neural engineering*, vol. 15, no. 6, pp. 066011, 2018.
- [20] Robin Tibor Schirmer, Jost Tobias Springenberg, Lukas Dominique Josef Fiederer, Martin Glasstetter, Katharina Eggensperger, Michael Tangermann, Frank Hutter, Wolfram Burgard, and Tonio Ball, "Deep learning with convolutional neural networks for eeg decoding and visualization," *Human brain mapping*, vol. 38, no. 11, pp. 5391–5420, 2017.
- [21] Michael Tangermann, Klaus-Robert Müller, Ad Aertsen, Niels Birbaumer, Christoph Braun, Clemens Brunner, Robert Leeb, Carsten Mehring, Kai J Miller, Gernot Mueller-Putz, et al., "Review of the bci competition iv," *Frontiers in neuroscience*, p. 55, 2012.
- [22] Hohyun Cho, Minkyu Ahn, Sangtae Ahn, Moonyoung Kwon, and Sung Chan Jun, "Eeg datasets for motor imagery brain-computer interface," *GigaScience*, vol. 6, no. 7, pp. gix034, 2017.
- [23] Ary L Goldberger, Luis AN Amaral, Leon Glass, Jeffrey M Hausdorff, Plamen Ch Ivanov, Roger G Mark, Joseph E Mietus, George B Moody, Chung-Kang Peng, and H Eugene Stanley, "Physiobank, physiotoolkit, and physionet: components of a new research resource for complex physiologic signals," *circulation*, vol. 101, no. 23, pp. e215–e220, 2000.
- [24] Bangyan Zhou, Xiaopei Wu, Zhao Lv, Lei Zhang, and Xiaojin Guo, "A fully automated trial selection method for optimization of motor imagery based brain-computer interface," *PLoS one*, vol. 11, no. 9, pp. e0162657, 2016.
- [25] Jaeyoung Shin, Alexander von Lüthmann, Benjamin Blankertz, Do-Won Kim, Jichai Jeong, Han-Jeong Hwang, and Klaus-Robert Müller, "Open access dataset for eeg+ mrs single-trial classification," *IEEE Transactions on Neural Systems and Rehabilitation Engineering*, vol. 25, no. 10, pp. 1735–1745, 2016.
- [26] Claire Cury, Giulia Lioi, Lorraine Perronnet, Anatole Lécuyer, Pierre Maurel, and Christian Barillot, "Impact of 1d and 2d visualisation on eeg-fMRI neurofeedback training during a motor imagery task," in *2020 IEEE 17th International Symposium on Biomedical Imaging (ISBI)*. IEEE, 2020, pp. 1018–1021.
- [27] He He and Dongrui Wu, "Transfer learning for brain-computer interfaces: A euclidean space data alignment approach," *IEEE Transactions on Biomedical Engineering*, vol. 67, no. 2, pp. 399–410, 2019.